IEEE Access
Multidisciplinary | Rapid Review | Open Access Journal

Received September 4, 2018, accepted October 11, 2018, date of publication November 9, 2018,
date of current version December 3, 2018.

*Digital Object Identifier 10.1109/ACCESS.2018.2876700*

# Understanding UAV Cellular Communications: From Existing Networks to Massive MIMO

**GIOVANNI GERACI[1], (Member, IEEE), ADRIAN GARCIA-RODRIGUEZ[2], (Member, IEEE), LORENZO GALATI GIORDANO[2], (Member, IEEE), DAVID LÓPEZ-PÉREZ[2], (Senior Member, IEEE), AND EMIL BJÖRNSON[3], (Senior Member, IEEE)**

[1]Department of Information and Communication Technologies, Universitat Pompeu Fabra, 08018 Barcelona, Spain
[2]Nokia Bell Labs, Dublin, D15 Y6NT Ireland
[3]Department of Electrical Engineering, Linköping University, 581 83 Linköping, Sweden

Corresponding author: Giovanni Geraci (dr.giovanni.geraci@gmail.com)

The work of G. Geraci was partly supported by the Postdoctoral Junior Leader Fellowship Programme from "la Caixa" Banking Foundation. The work of E. Björnson was supported by "ELLIIT and CENIIT."

**ABSTRACT** The purpose of this paper is to bestow the reader with a timely study of UAV cellular communications, bridging the gap between the 3GPP standardization status quo and the more forward-looking research. Special emphasis is placed on the downlink command and control (C&C) channel to aerial users, whose reliability is deemed of paramount technological importance for the commercial success of UAV cellular communications. Through a realistic side-by-side comparison of two network deployments – a present-day cellular infrastructure versus a next-generation massive MIMO system – a plurality of key facts are cast light upon, with the three main ones summarized as follows: 1) UAV cell selection is essentially driven by the secondary lobes of a base station's radiation pattern, causing UAVs to associate to far-flung cells; 2) over a 10 MHz bandwidth, and for UAV heights of up to 300 m, massive MIMO networks can support 100 kbps C&C channels in 74% of the cases when the uplink pilots for channel estimation are reused among base station sites, and in 96% of the cases without pilot reuse across the network; and 3) supporting UAV C&C channels can considerably affect the performance of ground users on account of severe pilot contamination, unless suitable power control policies are in place.

**INDEX TERMS** Unmanned aerial vehicles (UAVs), command and control channel, cellular networks, massive MIMO, 3GPP.

## I. INTRODUCTION

The latest proliferation of unmanned aerial vehicles (UAVs) – more commonly referred to as *drones* – is generating thrill, charm, and engagement in the public and private domains alike. Highly mobile UAVs are regarded as the best candidates to automate and ease emergency search-and-rescue missions, crowd management and surveillance, as well as weather and traffic monitoring [2], [3]. Their recently reduced cost also makes drones suitable for less critical applications such as package delivery and video streaming of breathtaking landscapes. All but unheard of until just recently, drones are now envisioned to shape the future of technology, providing a useful, trustworthy, and safe solution for human endeavors [4], [5]. Moreover, a rapid and vast growth in the UAV business will likely open attractive vertical markets in the telecommunications industry, bringing new revenue opportunities for mobile network vendors and operators.

### A. BACKGROUND AND MOTIVATION

For the above technological and commercial visions to turn into reality, UAV users will require control and connectivity over a wireless network. Solutions are urgently needed to transfer large amounts of data, e.g., video streaming generated by high-resolution cameras, from aerial users to ground base stations (BSs) [6]–[8]. More importantly, reliable command and control (C&C) channels to the UAVs are required to safely operate these vehicles remotely and beyond the visual line-of-sight (LoS) constraints currently enforced by regulatory bodies [9]. In this setup, terrestrial cellular networks are well suited to serve UAV users flying up to a height of few hundred meters.

Although connecting UAVs through cellular technologies has key potential advantages – such as enabling connectivity via existing network infrastructure and spectrum resources – it also involves important challenges. Indeed, UAVs may

undergo radio propagation characteristics that are profoundly different from those encountered by conventional ground users (GUEs). As they can move in three dimensions, UAVs could be placed in locations considerably above ground, experiencing a larger distance to the radio horizon and favorable LoS propagation conditions with a vast number of BSs [10]. As a result, a UAV transmitting uplink (UL) information to its serving BS could create significant interference to a plurality of neighboring BSs, receiving both GUE and UAV UL transmissions. Conversely, BSs communicating with their GUEs or UAVs in downlink (DL) could severely disrupt the DL of a UAV associated to a neighboring BS [11], [12].

In light of these challenges, and with the aim of integrating UAV communications in current cellular networks, the Third Generation Partnership Project (3GPP) has been gathering key industrial players to collaborate on a *study item* on enhanced LTE support for aerial vehicles. Notably, such joint effort – that has just reached its conclusion, and that has been followed by the corresponding *work item* – has produced systematic measurements and accurate UAV-to-ground channel modeling [8]. Furthermore, it has defined the various UAV link types along with their respective features and minimum requirements, as summarized in Table 1. The remarkable industrial involvement in UAV cellular communications standardization [13]–[18], together with the concurrent theoretical investigations undertaken by academia [19]–[24], prompt us to bridge the gap and provide a compelling study that follows the most recent 3GPP recommendations and sets the trend for present-and-forward-looking research.

**TABLE 1. Taxonomy of UAV link types.**

| | Link Type | Data Rate | Critical? |
|---|---|---|---|
| DL | Synchronization (PSS/SSS) | N/A | ✓ |
| | Radio control (PDCCH) | | ✓ |
| | C&C | 60-100 kbps | ✓ |
| UL | C&C | 60-100 kbps | ✓ |
| | Payload | Best effort | ✗ |

### B. APPROACH AND SUMMARY OF RESULTS

The goal of this paper is to advance the understanding of UAV cellular communications, placing emphasis on the performance of the UAV DL C&C channel, for which the 3GPP has defined a minimum requirement of 100 kbps [8].[1] Such focus is motivated by the pursuit of mobile operators for new market shares. Unlike UAV payload traffic, potentially similar to – and in lower amount than – current data traffic, handling C&C traffic could yield additional profits that may justify investments to upgrade the network infrastructure. In light of this prospect, we extend our study to two network architectures, both operating on a 10 MHz bandwidth: *(i)* a traditional cellular network with three-sector BSs operating in *single-user* mode (i.e., one user scheduled per frequency-time resource at a time) – representing most existing deployments; and *(ii)* a massive MIMO cellular deployment operating in *multi-user* mode (i.e., multiple users scheduled per frequency-time resource) capable of digital beamforming – exemplifying next-generation networks.

For the above two practical setups, we closely examine how the height of a UAV user affects its cell selection process and its performance. We then evaluate the increased reliability that can be achieved for the UAV C&C channel with massive MIMO, also quantifying what the UAV presence entails for the performance of conventional GUEs. While we refer the reader to the body of the article for a comprehensive collection of results and discussions, the following list serves as a preview of the most important takeaways of our study:

- For UAV heights of 75 m and above, due to an almost free-space propagation, cell selection in existing networks is mostly driven by the secondary lobes of each BS's antenna pattern, rather than by the path loss difference among BSs. Hence, UAVs do not generally associate to BSs located nearby but to those found farther away.
- In current single-user mode networks designed for GUEs, UAVs that take off or land at 1.5 m meet the C&C target rate of 100 kbps in 87% of the cases. However, owing to strong LoS interference received from a plurality of cells, such reliability drops to 35% at 50 m, and to a mere 2% and 1% respectively at 150 m and 300 m.
- Massive MIMO can support a 100 kbps UAV C&C channel for heights up to 300 m with 74% and 96% reliability, respectively with and without pilot reuse three and contamination. This is due to a stronger carrier signal, a mitigated interference, and a spatial multiplexing gain.
- The presence of UAVs can severely degrade the performance achieved by GUEs under massive MIMO. An UL power control policy is required to protect GUEs whose pilot signals are otherwise vulnerable to significant contamination from UAV-generated overlapping pilots.

### C. TARGET AUDIENCE

*Who should read this paper?* We trust at least two categories of readers will find this article worthy of their attention:

- Industrial innovators, wondering whether – and to what extent – UAV users could be supported by present-day networks and by upcoming massive MIMO deployments.
- Academic researchers, pursuing an analysis of real-world phenomena occurring in UAV communications.

Readers in the former group may value the efforts we made in implementing with utmost accuracy the latest standardized air-to-ground propagation channel models and system parameters. They may also acknowledge the care we took in selecting and explaining the results of our extensive system-level simulation campaigns. While our quest for

[1] An evaluation of the UL data rates is underway, and readers are referred to [25] for a preview. Though studying the UL and DL latency is complementary and on our roadmap, it falls beyond the scope of the present article.

accuracy compelled us to forgo analytical tractability, we hope this study will also entice academia. May our findings motivate such readership to reproduce them through theoretical analysis, and to propose breakthroughs that improve cellular support for UAV users.

## II. 3GPP SYSTEM SETUP

In this section, we introduce the 3GPP network topology and channel model employed. Further details on the parameters used in our study are given in Table 2.[2]

**TABLE 2. System parameters.**

| | |
|---|---|
| **Deployment** | |
| BS distribution | Three-tier wrapped-around hexagonal grid, 37 sites, three sectors each, one BS per sector [8] |
| BS inter-site distance | 500 m [8] |
| User distribution | 15 users per sector on average [8] |
| GUE distribution | 80% indoor, horizontal: uniform, vertical: uniform in buildings of four to eight floors |
| | 20% outdoor, horizontal: uniform, vertical: 1.5 m |
| UAV distribution | 100% outdoor, horizontal: uniform, vertical: uniform between 1.5 m and 300 m [8] |
| UAVs/GUEs ratio | 3GPP Case 3: 7.1%, Case 4: 25%, Case 5: 50% [8] |
| User association | Based on RSRP (large-scale fading) |
| **Channel model** | |
| Path loss | Urban Macro as per [8], [29] |
| Probability of LoS | Urban Macro as per [8], [29] |
| Shadow fading | Urban Macro as per [8], [29] |
| Small-scale fading | Urban Macro as per [8], [29] |
| Channel estimation | Single-user: perfect channel estimation |
| | Multi-user: UL SRSs with Reuse 3 |
| Thermal noise | -174 dBm/Hz spectral density [8] |
| **PHY** | |
| Carrier frequency | 2 GHz [8] |
| System bandwidth | 10 MHz with 50 PRBs [8] |
| BS transmit power | 46 dBm [8] |
| BS antenna elements | Horizontal and vertical half power beamwidth: 65°, max. gain: 8 dBi [8] |
| BS array configuration | Height: 25 m, mechanical downtilt: 12°, element spacing: $0.5\lambda$ [8] |
| BS array size | Single-user: $8 \times 1$ X-POL $\pm 45°$, 1 RF chain |
| | Multi-user: $8 \times 8$ X-POL $\pm 45°$, 128 RF chains |
| BS precoder | Single-user: none |
| | Multi-user: zero-forcing |
| Power control | DL: equal power allocation |
| | UL: fractional power control with $\alpha = 0.5$, $P_0 = -58$ dBm, and $P_{\max} = 23$ dBm [30] |
| User antenna | Omnidirectional with vertical polarization, gain: 0 dBi [8] |
| Noise figure | BS: 7 dB, user: 9 dB [8], [31] |
| **MAC** | |
| Traffic model | Full buffer |
| Scheduler | Single-user: round-robin [32], one user per PRB |
| | Multi-user: round-robin, eight users per PRB |

### A. CELLULAR NETWORK TOPOLOGY

We consider the DL of a traditional cellular network (designed for GUEs) as depicted in Fig. 1, where BSs are deployed on a hexagonal layout and communicate with their respective sets of connected users. Each deployment site is comprised of three co-located BSs, each covering one sector spanning an angular interval of 120°. Unlike conventional networks, the cellular network under consideration serves both GUEs and UAVs, e.g., providing GUEs with DL data streams and UAVs with C&C information. In what follows, *users* denotes both GUEs and UAVs. GUEs are located both outdoor (at a height of 1.5 m) and indoor in buildings that consist of several floors. UAVs are located outdoor at variable heights between 1.5 m, which represents their height during take off and landing, and 300 m, which is regarded as their maximum cruising altitude with cellular service.[3] All deployment features comply with the ones specified by the 3GPP in [8].

The set of cellular BSs is denoted by $\mathcal{B}$, and we assume that all BSs transmit with total power $P_{\mathrm{B}}$. The transmission power per time-frequency physical resource block (PRB) is given by $P_{\mathrm{b}} = P_{\mathrm{B}}/F$, where $F$ denotes the total number of PRBs. Users associate to the BS providing the largest reference signal received power (RSRP) across the whole communication band. Each BS is equipped with $N_{\mathrm{a}}$ antennas, and we assume all users to be equipped with a single antenna. We denote as $\mathcal{K}_b$ the set of users served by BS $b$ on a given PRB, and by $K_b$ its cardinality. While the total number of associated users is determined by their density and distribution, the set $\mathcal{K}_b$ can be chosen adaptively by BS $b$ through scheduling operations. In this regard, we identify two cases: the one where $K_b = 1$ (*single-user* mode operations) and the one where $K_b \geq 1$ (*multi-user* operations through spatial multiplexing). These two cases are illustrated in Fig. 1(a) and Fig. 1(b), and will be addressed in Sec. III and Sec. IV, respectively.

### B. 3D PROPAGATION CHANNEL MODEL

We adopt the latest 3GPP channel model for evaluating cellular support for UAVs [8]. In this model, all radio links are affected by large-scale fading (comprising antenna gain, path loss, and shadow fading) and small-scale fading. Among other real-world phenomena, the model accounts for 3D channel directionality, spatially correlated shadowing, and time-and-frequency correlated small-scale fading. Moreover, all propagation parameters for aerial devices in the model – such as path loss, probability of LoS, shadow fading, and small-scale fading – have been derived as a result of numerous measurement campaigns, and explicitly account for the transmitter and receiver heights.

On a given PRB, $\mathbf{h}_{bjk} \in \mathbb{C}^{N_{\mathrm{a}} \times 1}$ denotes the channel vector between BS $b$ and user $k$ in cell $j$. The signal $y_{bk} \in \mathbb{C}$ received

[2] As reporting the entire channel model would require an article on its own, readers are referred to [8] for any information not contained in Table 2.

[3] While studying the implications of mobility is on our roadmap, in this paper we consider static UAVs to isolate and evaluate the impact of their altitude on performance. Readers interested in the effect of mobility (e.g., on handovers) are referred to [26] and [27].

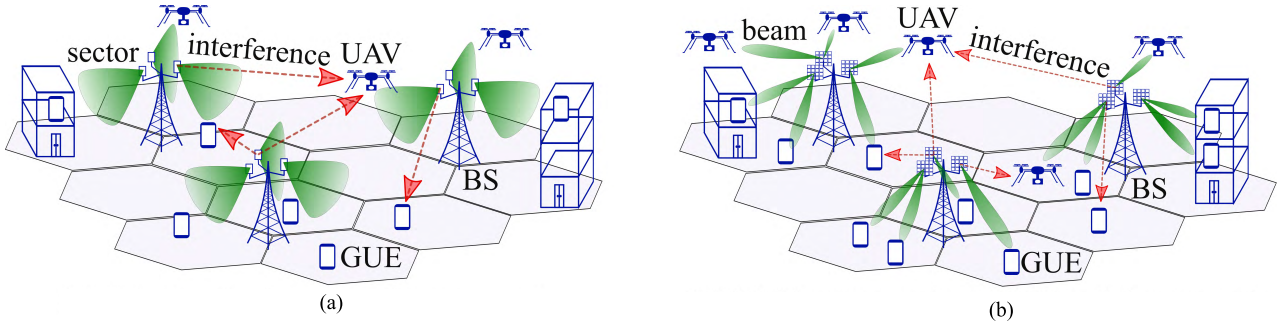


**FIGURE 1.** Two examples of cellular infrastructure for supporting both ground and UAV users. In (a) – similarly to many existing deployments – BSs cover a cellular sector with a vertical antenna panel and serve a single user on each PRB, potentially generating strong interference towards nearby users. In (b) – which exemplifies next-generation deployments – BSs serve multiple users on each PRB through massive MIMO arrays and beamforming; this increases the useful signal power at each served user, and mitigates the interference towards nearby users.

by user $k$ in cell $b$ can be expressed as

$$y_{bk} = \sqrt{P_\mathrm{b}}\,\mathbf{h}_{bbk}^\mathrm{H}\mathbf{w}_{bk}s_{bk} + \sqrt{P_\mathrm{b}}\sum_{i\in\mathcal{K}_b\setminus k}\mathbf{h}_{bbk}^\mathrm{H}\mathbf{w}_{bi}s_{bi} + \sqrt{P_\mathrm{b}}\sum_{j\in\mathcal{B}\setminus b}\sum_{i\in\mathcal{K}_j}\mathbf{h}_{jbk}^\mathrm{H}\mathbf{w}_{ji}s_{ji} + \epsilon_{bk}, \quad (1)$$

where $s_{bk} \in \mathbb{C}$ is the unit-variance signal intended for user $k$ in cell $b$, $\epsilon_{bk} \sim \mathcal{CN}(0, \sigma_\epsilon^2)$ is the thermal noise, and $\mathbf{w}_{bk} \in \mathbb{C}^{N_\mathrm{a}\times 1}$ is the transmit precoding employed by BS $b$ to serve user $k$ in cell $b$. The latter is normalized to satisfy the total power constraint, and it is assumed to be a vector of identical scalars for single-user mode operations (representing an analog signal combiner without phase shifters), and a digital zero-forcing (ZF) precoder for multi-user operations, as detailed in Sec. III and Sec. IV, respectively. The four terms on the right hand side of (1) respectively represent: the useful signal, the intra-cell interference from the serving BS (only present for multi-user operations), the inter-cell interference from other BSs, and the thermal noise.

Assuming that the users have perfect channel state information (CSI), the resulting instantaneous signal-to-interference-plus-noise ratio (SINR) $\gamma_{bk}$ at user $k$ in cell $b$ on a given PRB is obtained as an expectation over all symbols, and it is given by

$$\gamma_{bk} = \frac{P_\mathrm{b}\,|\mathbf{h}_{bbk}^\mathrm{H}\mathbf{w}_{bk}|^2}{P_\mathrm{b}\sum\limits_{i\in\mathcal{K}_b\setminus k}|\mathbf{h}_{bbk}^\mathrm{H}\mathbf{w}_{bi}|^2 + P_\mathrm{b}\sum\limits_{j\in\mathcal{B}\setminus b}\sum\limits_{i\in\mathcal{K}_j}|\mathbf{h}_{jbk}^\mathrm{H}\mathbf{w}_{ji}|^2 + \sigma_\epsilon^2}. \quad (2)$$

Each value of SINR is mapped to the rate achievable on a given PRB by assuming ideal link adaptation, i.e., choosing the maximum modulation and coding scheme (MCS) that yields a desired block error rate (BLER) [28]. We set the BLER to $10^{-1}$, which we regard as a sufficiently low value considering that retransmissions further reduce the number of errors. This yields minimum and maximum spectral efficiencies of 0.22 b/s/Hz and 7.44 b/s/Hz, for SINRs in the range $[-5.02$ dB, $-4.12$ dB$]$ and $[25.87$ dB, $+\infty]$, respectively. When computing the achievable rates, we also account for the overhead due to control signaling [28].

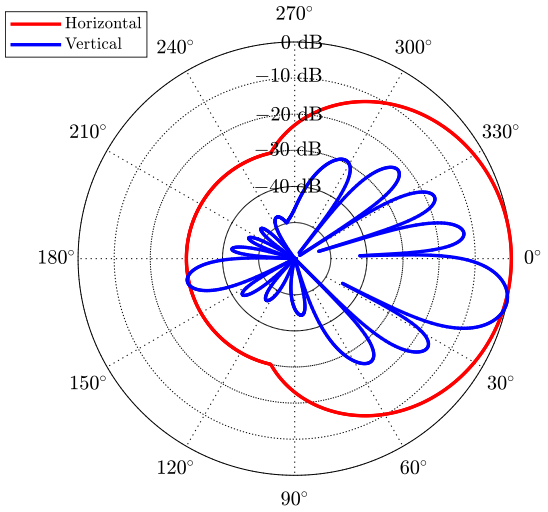


**FIGURE 2.** Horizontal and vertical antenna pattern (normalized to maximum gain) of a BS consisting of a vertical array of 8 X-POL elements, each with 65° half power beamwidth, mechanically downtilted by 12°.

## III. INTEGRATING UAVs INTO EXISTING NETWORKS

In this section, we consider the cellular network depicted in Fig. 1(a), where each BS is equipped with $N_\mathrm{a} = 16$ antennas arranged in a vertical array of 8 cross-polarized (X-POL) elements, each with 65° half power beamwidth, mechanically downtilted by 12° and supported by a single radio-frequency (RF) chain. Such configuration yields the BS antenna pattern depicted in Fig. 2. In this setup, each BS serves at most one user on each PRB, without employing digital precoding [31], [33], [34]. Such setup embodies current cellular networks, and we refer to it as *single-user* mode. In this mode, equations (1) and (2) simplify as follows: all precoding vectors $\mathbf{w}$ consist of identical scalars, the second term on the right hand side of (1) vanishes, and so does the first one in the denominator of (2). For this setup, we will closely examine how a UAV's height affect its serving BS selection and its DL C&C channel performance.

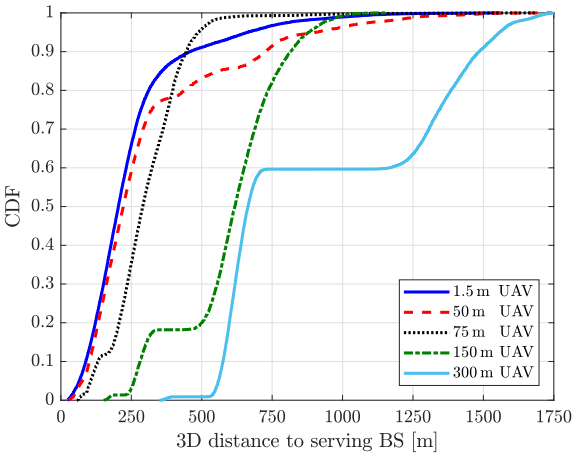


**FIGURE 3.** CDF of the 3D distance between a UAV and its serving BS in an existing cellular network. Various UAV heights are considered.

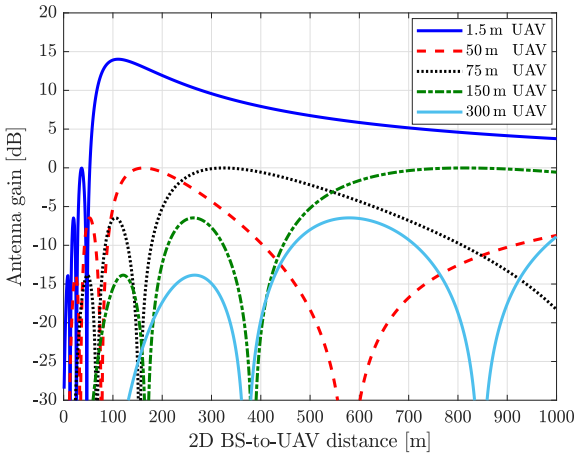


**FIGURE 4.** Antenna gain between a BS in an existing cellular network and a UAV aligned to the BS's horizontal bearing as a function of their 2D distance. Various UAV heights are considered.

### *A. UAV ASSOCIATION*

Fig. 3 shows the cumulative distribution function (CDF) of the 3D distance between a UAV and its best potential serving BS for data transmission and reception. The CDF of said distance is plotted for UAV heights of 1.5 m, 50 m, 75 m, 150 m, and 300 m. For the same set of heights, Fig. 4 illustrates the antenna gain between a BS and a UAV aligned to the BS's horizontal bearing versus their mutual 2D ground distance. By jointly looking at these two figures, three association behaviors can be clearly identified for different UAV heights.

#### 1) UAVs AT 1.5 m

UAVs at the same height as outdoor GUEs exhibit an association distance smoothly distributed between 35 m and 1 km (Fig. 3). By recalling that the inter-site distance is 500 m, one can make the two following observations:

- A UAV at 1.5 m is captured by the main lobe of a BS as long as their mutual 2D distance exceeds 52 m (Fig. 4). Moreover, the antenna gain is maximized for 2D distances between 80 m-180 m (Fig. 4), hence selections of BSs other than the nearest one are mostly due to shadowing and LoS conditions.
- UAVs at 1.5 m generally associate to their closest BS – i.e., at a distance up to around 250 m (Fig. 3). Association to BSs located at a distance of 500 m or more occurs only in 9% of the cases (Fig. 3).

#### 2) UAVs AT 50 m

For UAVs flying at this moderate height, one can find similarities as well as differences with respect to the previous case of low-height UAVs:

- For 3D distances of 250 m or less, the CDFs in Fig. 3 reveal similar behavior when comparing a UAV at 1.5 m with one at 50 m. Such similarity can be explained from the fact that the vertical distance to a BS – standing at 25 m – is similar for the two UAVs. This implies that a BS sees the two UAVs with a similar angle (slightly better for the 1.5 m UAV due to the 12° BS antenna downtilt), and that the antenna gain as a function of the 2D distance follows a similar pattern (Fig. 4).
- For 3D distances of more than 250 m, the two CDFs in Fig. 3 exhibit a different behavior. Indeed, UAVs at 50 m are more likely to associate to BSs located 500 m away compared to UAVs at 1.5 m (in 17% of the cases as opposed to 9% of the cases). This can be explained by looking at the difference in the two antenna gain trends (Fig. 4). The higher likelihood of seeing multiple neighboring BSs in LoS for 50 m-high UAVs also contributes to the above phenomenon.

#### 3) UAVs AT 75 m AND ABOVE

As the height of a UAV increases to 75 m and beyond, not only the association distance grows, but also its CDF exhibits a certain number of steps, each corresponding to a different association distance range (Fig. 3). Such distance ranges are clearly separated from one another, and are due to the secondary lobes of each BS's antenna pattern (see Fig. 2). Indeed, when UAVs fly very high, the main BS antenna lobe is visible only at 2D distances larger than 1 km (beyond the range of Fig. 4). Side lobes therefore play a crucial part in the association process. Due to an almost free-space propagation, the difference in path loss between the nearest and the farther BSs is less significant than the difference in their respective antenna gains [8]. As a result, UAVs tend to select BSs located at large distances with better secondary lobe gains.

The above phenomena are further illustrated in Fig. 5. This figure takes the point of view of a three-sector BS placed at the origin, showing samples of the 2D locations of the associated UAVs for UAV heights of 150 m (red dots). Fig. 5 shows the existence of distance intervals (highlighted in green), each corresponding to one of the CDF steps in Fig. 3 or, equivalently, to one of the side lobes in Fig. 2 and Fig. 4.

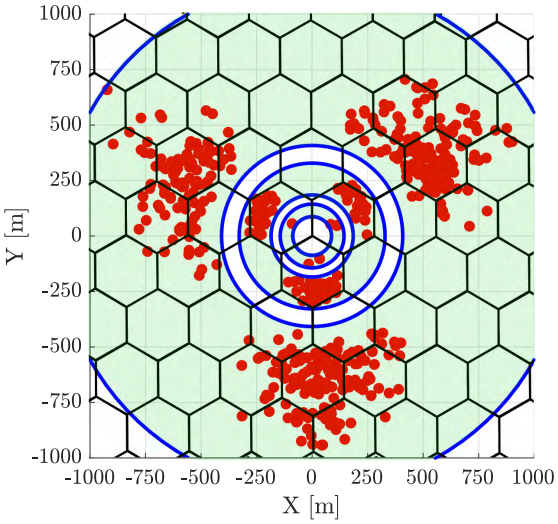


**FIGURE 5.** Red dots represent the 2D location of 150 m-high UAVs associated to a three-sector BS site placed at the origin. Distance intervals corresponding to different side lobes are shaded and delimited by blue circles.

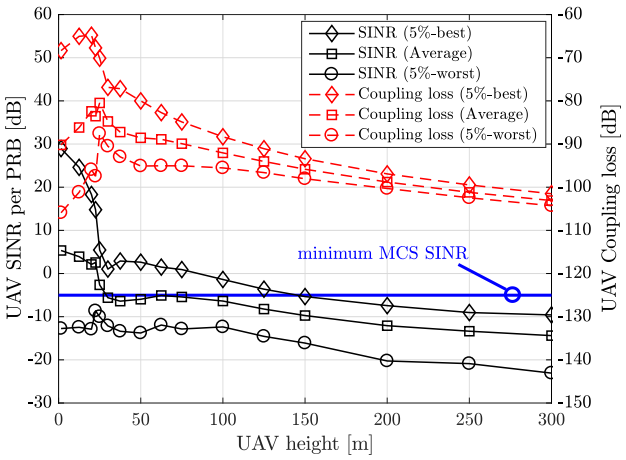


**FIGURE 6.** Coupling loss (right y-axis) and SINR per PRB (left y-axis) experienced by a UAV versus its height in a single-user scenario. The minimum MCS SINR threshold of −5.02 dB is also shown as a benchmark.

### B. UAV C&C CHANNEL PERFORMANCE

#### 1) CARRIER SIGNAL STRENGTH AND INTERFERENCE

Six curves are plotted in Fig. 6 in order to show the coupling loss and the SINR per PRB experienced by a UAV as a function of its height. The coupling loss (right y-axis) expresses the carrier signal attenuation between the serving BS and a UAV due to antenna gain, path loss, and shadow fading. On the other hand, the SINR per PRB (left y-axis) also accounts for small-scale fading and for the interference perceived at the UAV. For both metrics, Fig. 6 shows the 5%-best (i.e., 95%-ile), average, and 5%-worst values, triggering the following observations:

- As UAVs rise from the ground up to a height of around 25 m, their average coupling loss improves due to closer proximity to the serving BS and increased probability of experiencing a LoS link with the latter. Instead, the 5%-best UAVs, which were those located in the direction of the main lobe of the BSs, experience a degraded coupling loss as a consequence of a diminished antenna gain. As the UAV height keeps increasing, so does the BS-to-UAV distance, causing the coupling loss to decay.
- While the average UAV coupling loss is moderately improved, a UAV flying at around 25 m generally sees a degraded SINR per PRB. This is caused by the fact that more neighboring BSs become visible to the UAV, acting as strong LoS interferers. The opposite occurs for the 5%-worst UAVs flying at 25 m, which experience a significant improvement in their coupling loss, and as a result, also enhance their SINR. As the UAV height keeps increasing, the SINR keeps decreasing, though more slowly than the coupling loss. This trend is due to a simultaneous slight reduction of the interference as the UAV moves further away from neighboring interfering BSs.
- Overall, UAVs flying at heights of 25 m and above experience low values of SINR per PRB. In particular, for heights beyond 100 m the average SINR falls below the minimum MCS SINR threshold of -5.02 dB; for heights beyond 150 m even the 5%-best SINR per PRB falls below said minimum threshold.[4]

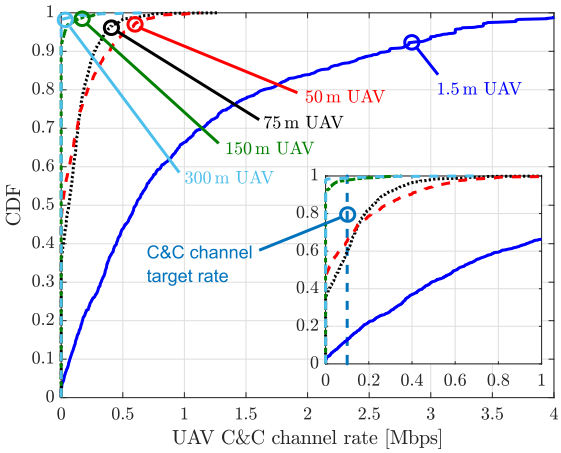


**FIGURE 7.** CDF of the UAV C&C channel rates versus the UAV height in single-user mode. The target rate of 100 kbps is also shown in the enlargement.

#### 2) C&C CHANNEL DATA RATES

The measured values of SINR per PRB can be translated into the data rate performance of the UAV C&C channel over a 10 MHz bandwidth, as per the MCS selection described in Sec. II. Fig. 7 shows said performance for several UAV

[4]In practice, opportunistic proportional-fair schedulers could be employed that outperform the round-robin scheduler considered in this paper. However, this measure alone would not suffice to bring the UAV C&C channel performance to an acceptable level in single-user mode networks. Indeed, Fig. 6 shows that even the 5%-best UAVs, which corresponds to those with large channel fading gains, experience very low values of SINR.

heights, motivating the following conclusions: The measured values of SINR per PRB can be translated into the data rate performance of the UAV C&C channel over a 10 MHz bandwidth, as per the MCS selection described in Sec. II. Fig. 7 shows said performance for several UAV heights, motivating the following conclusions:

- UAVs at 1.5 m meet the target rate of 100 kbps 87% of the time, and 34% of the time their rates even exceed 1 Mbps.
- UAVs at around 50 m and 75 m respectively achieve the target rate 35% and 40% of the time only. The achievable rates for this range of heights almost never reach 1 Mbps (0.3% of the time).
- At higher heights, the UAV target rate of 100 kbps can only be achieved for small fractions of time, amounting to just 2% and 1% for heights of 150 m and 300 m, respectively.

The above results prompt us to conclude that in cellular networks with heavy data traffic, simply relying on BS sectorization and single-user mode operations may not be sufficient to support the much-needed C&C channel for UAVs flying at reasonable heights.[5]

## IV. SUPPORTING UAVs THROUGH MASSIVE MIMO

In this section, we consider a network as depicted in Fig. 1(b), where cellular BSs are equipped with massive MIMO antenna arrays and avail of beamforming and spatial multiplexing capabilities. In particular, we consider $N_{\mathrm{a}} = 128$ antennas, arranged in an $8 \times 8$ planar array of $\pm 45°$ cross-polarized elements, fed by 128 RF chains. As massive MIMO enables the transmission of beamformed control channels towards each user, users tend to associate to a nearby BS. We allow each BS $b$ to serve at most $K_b = 8$ users per PRB via digital ZF precoding.[6] We denote this setup as a *multi-user* mode scenario, and we consider it as an embodiment of next-generation massive MIMO cellular deployments. In such multi-user mode setting, the network operates in a time-division duplexing (TDD) fashion, where channels are estimated at the BS via UL sounding reference signals (SRSs) – commonly known as *pilots* – sent by the users under the assumption of channel reciprocity [36]. In the following, we describe in detail the sequence of operations performed in this multi-user system.

### 1) CHANNEL STATE INFORMATION ACQUISITION

Let the pilot signals span $M_{\mathrm{p}}$ symbols. The pilot transmitted by user $k$ in cell $b$ is denoted by $\mathbf{v}_{\mathrm{i}_{bk}} \in \mathbb{C}^{M_{\mathrm{p}}}$, where $\mathrm{i}_{bk}$ is the index in the pilot codebook, and all pilots in the codebook form an orthonormal basis [36]. Each pilot signal received at the BS undergoes *contamination* due to pilot reuse across cells. We assume pilot Reuse 3, i.e., the set of pilot signals is orthogonal among the three 120° BS sectors of the same site, but it is reused among all BS sites, creating contamination. This solution is particularly practical from an implementation perspective, since it involves coordination only between the three co-located BSs of the same site. Each BS sector randomly allocates its pool of pilots to its served users. The collective received signal at BS $b$ is denoted as $\mathbf{Y}_b \in \mathbb{C}^{N_{\mathrm{a}} \times M_{\mathrm{p}}}$, and given by

$$\mathbf{Y}_b = \sum_{j \in \mathcal{B}} \sum_{k \in \mathcal{K}_j} \sqrt{P_{jk}} \mathbf{h}_{bjk} \mathbf{v}_{\mathrm{i}_{jk}}^{\mathrm{T}} + \mathbf{N}_b, \tag{3}$$

where $\mathbf{N}_b$ contains the additive noise at BS $b$ during pilot signaling with independent and identically distributed entries following $\mathcal{CN}(0, \sigma_\epsilon^2)$, and $P_{jk}$ is the power transmitted by user $k$ in cell $j$. We assume fractional UL power control as follows [30]

$$P_{jk} = \min \left\{ P_{\max}, P_0 \cdot \bar{h}_{jjk}^{\alpha} \right\}, \tag{4}$$

where $P_{\max}$ is the maximum user transmit power, $P_0$ is a cell-specific parameter, $\alpha$ is a path loss compensation factor, and $\bar{h}_{jjk}$ is the average channel gain measured at UE $k$ in cell $j$ based on the RSRP [28], [37]. The aim of (4) is to compensate only for a fraction $\alpha$ of the path loss, up to a limit specified by $P_{\max}$.

The received signal $\mathbf{Y}_b$ in (3) is processed at BS $b$ by correlating it with the known pilot signal $\mathbf{v}_{\mathrm{i}_{bk}}$, thus rejecting interference from other orthogonal pilots. BS $b$ hence obtains the following least-squares channel estimate for user $k$ in cell $b$ [38]

$$\begin{aligned} \widehat{\mathbf{h}}_{bbk} &= \frac{1}{\sqrt{P_{bk}}} \mathbf{Y}_b \mathbf{v}_{\mathrm{i}_{bk}}^{*} \\ &= \mathbf{h}_{bbk} + \frac{1}{\sqrt{P_{bk}}} \Big( \sum_{j \in \mathcal{B} \setminus b} \sum_{k' \in \mathcal{K}_j} \sqrt{P_{jk'}} \mathbf{h}_{ijk'} \mathbf{v}_{\mathrm{i}_{jk'}}^{\mathrm{T}} + \mathbf{N}_i \Big) \mathbf{v}_{\mathrm{i}_{bk}}^{*} \end{aligned} \tag{5}$$

where intra-cell pilot contamination is not present since BS $b$ allocates orthogonal pilots for the users in its own cell.

### 2) SPATIAL MULTIPLEXING THROUGH DIGITAL PRECODING

Each BS simultaneously serves multiple users on each PRB via ZF precoding, attempting to suppress all intra-cell interference.[7] Let us define the estimated channel matrix $\widehat{\mathbf{H}}_b \in \mathbb{C}^{N_{\mathrm{a}} \times K_b}$ as

$$\widehat{\mathbf{H}}_b = \left[ \widehat{\mathbf{h}}_{bb1}, \ldots, \widehat{\mathbf{h}}_{bbK_b} \right]. \tag{6}$$

The ZF precoder

$$\mathbf{W}_b = \left[ \mathbf{w}_{b1}, \ldots, \mathbf{w}_{bK_b} \right] \tag{7}$$

at BS $b$ can be calculated as [39]

$$\mathbf{W}_b = \widehat{\mathbf{H}}_b \left( \widehat{\mathbf{H}}_b^{\mathrm{H}} \widehat{\mathbf{H}}_b \right)^{-1} (\mathbf{D}_b)^{-\frac{1}{2}}, \tag{8}$$

[5] While there is a strong interest in reusing the existing network infrastructure with downtilted antenna arrays, dedicated BSs with uptilted arrays could be considered in the future to provide C&C and connectivity just to UAVs.

[6] Scheduling a larger number of users may yield higher cell spectral efficiency. However, it may prevent achieving a minimum guaranteed rate for all users [35], which is the primary goal for DL UAV communications.

[7] We discuss inter-cell interference suppression techniques in Sec. V.

where the diagonal matrix $\mathbf{D}_b$ is chosen to meet the transmit power constraint with equal user power allocation,[8] i.e., $\|\mathbf{w}_{bk}\|^2 = P_b/K_b \ \forall k, b$. The SINR on a given PRB for user $k$ can be obtained from (2) with the precoding vectors $\mathbf{w}_{bk}$ as in (7).

In the remainder of this section, we will *A)* evaluate the UAV C&C channel performance improvement achieved through massive MIMO, and *B)* study what the UAV presence entails for the GUEs performance.

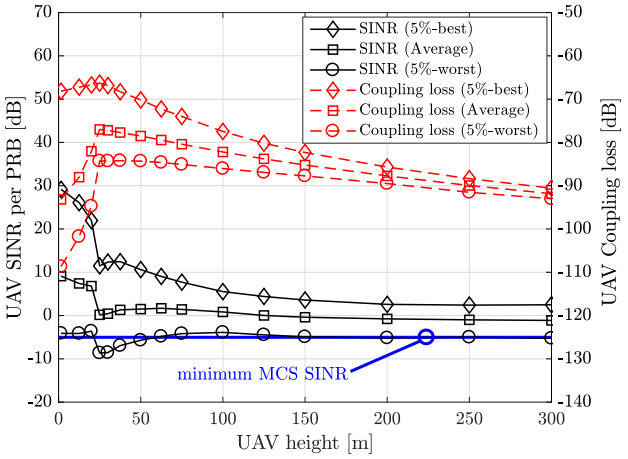


**FIGURE 8.** Coupling loss (right y-axis) and SINR per PRB (left y-axis) experienced by a UAV versus its height in a multi-user setup with perfect CSI (Case 3). The minimum MCS SINR threshold of -5.02 dB is also shown as a benchmark.

### A. UAV C&C CHANNEL PERFORMANCE IMPROVEMENT

Similarly to Fig. 6 and Fig. 7 for the single-user mode case, we now show the coupling loss (Fig. 8, right y-axis), SINR per PRB (Fig. 8, left y-axis), and C&C data rate (Fig. 9) achieved by a UAV as a function of its height in a multi-user massive MIMO setup. Both Fig. 8 and Fig. 9 consider the 3GPP Case 3, i.e., one UAV and 14 GUEs per sector [8]. In order to evaluate the gains theoretically achievable with massive MIMO, in these figures the BS is assumed to avail of perfect CSI, i.e., no pilot contamination is considered. A more realistic channel estimation through SRSs as in (5) and the effect of pilot contamination on the performance of both UAVs and GUEs will be thoroughly discussed in Sec. IV-B.

#### 1) CARRIER SIGNAL STRENGTH AND INTERFERENCE

Comparing Fig. 8 to Fig. 6 provides the following insights:

- Consistently with Fig. 6, a UAV flying at around 25 m generally sees an improved coupling loss but a degraded SINR per PRB. This is due to the fact that more neighboring BSs become visible to the UAV, acting as strong LoS interferers.
- Employing massive MIMO at the BSs while keeping the same mechanical downtilt improves the UAVs' coupling loss, which is measured at the output of the first RF chain [29], thanks to an increased antenna gain towards the sky.
- The SINR per PRB experienced by a UAV is largely improved in a massive MIMO system, owing to two phenomena. First, UAVs benefits from a beamforming gain from the serving BS, which can now send beams into the sky as well. Second, since most users are GUEs, neighboring BSs tend to point most of their beams downwards, greatly mitigating the interference generated at the UAVs.
- Overall, most UAVs experience values of SINR per PRB above the minimum MCS threshold. In particular, the average SINR per PRB is well above said threshold for any UAV height. Moreover, even the 5%-worst UAVs meet the minimum SINR threshold for most UAV heights.

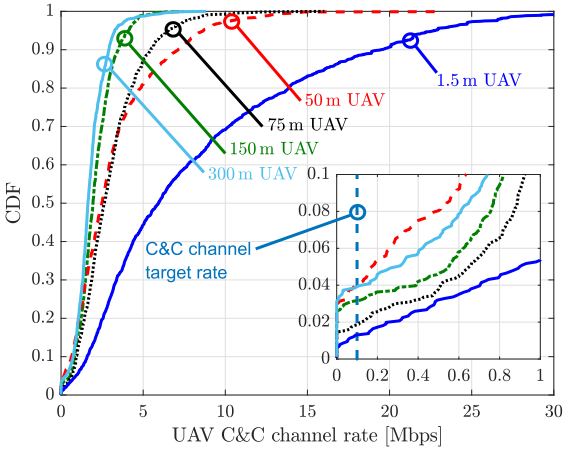


**FIGURE 9.** CDF of the UAV C&C channel rates for various UAV heights in a multi-user setup with perfect CSI (Case 3). The enlargement shows the target rate of 100 kbps as a benchmark.

#### 2) C&C CHANNEL DATA RATES

Fig. 9 shows the data rate performance of the UAV C&C channel in a multi-user massive MIMO setup for various UAV heights. Comparing this figure to Fig. 7 provides the reader with a key takeaway: unlike single-user mode cellular networks, massive MIMO networks have the potential to support a 100 kbps UAV C&C channel with good reliability, namely in at least 96% of the cases for all UAV heights under consideration. Indeed, the data rates in a massive MIMO network are largely improved owing to both an SINR gain (as per Fig. 8) and a spatial multiplexing gain owing to the fact that eight users, between UAVs and GUEs, are allocated the same PRB simultaneously.

### B. PERFORMANCE INTERPLAY BETWEEN UAVs AND GROUND USERS

We now study how supporting the UAV C&C channel through cellular networks may affect the performance of GUEs. In particular, we assess the impact of UAVs in both

[8]More sophisticated power allocation policies – e.g., max-min SINR – may be considered to further improve the performance of the worst UAVs.

single-user and multi-user mode settings with the user height distributions specified in Table 2. For the latter, we discuss the impact of SRS reuse and contamination, as well as the impact of UL power control in the channel estimation phase.

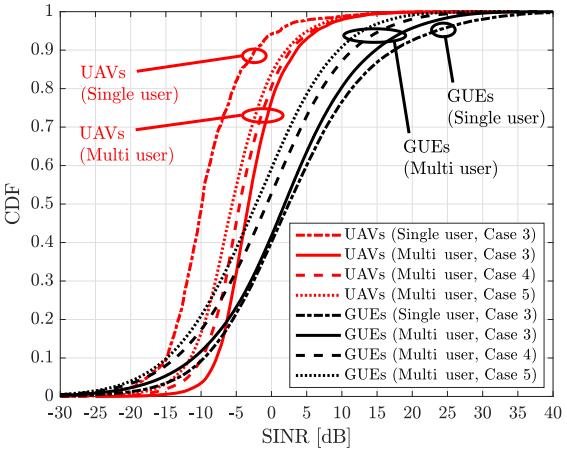


**FIGURE 10.** SINR per PRB experienced by UAVs and GUEs in single-user and multi-user scenarios with pilot Reuse 3 and UL fractional power control (various 3GPP cases).

### 1) 3GPP CASE STUDIES

Fig. 10 shows the SINR per PRB for both UAVs and GUEs in the presence of realistic CSI acquisition with SRS Reuse 3 and UL fractional power control. The figure considers the 3GPP Cases 3, 4, and 5, corresponding to one UAV and 14 GUEs, three UAVs and 12 GUEs, and five UAVs and 10 GUEs per sector, respectively. Fig. 10 carries multiple consequential messages:

- In spite of an imperfect CSI available at the BSs, the UAV SINR per PRB greatly improves when moving from a single-user to a multi-user mode scenario. This is due to a beamforming gain paired with a reduced interference from nearby BSs that focus most of their energy downwards.
- In line with the above, the UAV SINR per PRB in multi-user mode scenarios is reduced when moving from Case 3 to Cases 4 and 5, mainly because *(i)* a larger number of UAVs leads to an increased CSI pilot contamination due to their strong LoS channel to many BSs, and *(ii)* neighboring cells point more beams upwards, thus generating more inter-cell interference at the UAVs. On the other hand – although not explicitly shown in the figure – the number of UAVs does not affect the SINR in single-user mode scenarios.
- Unlike the UAV SINR, the GUE SINR does not improve when moving from a single-user to a multi-user scenario. This is mainly due to the severe pilot contamination incurred by GUEs, which outweighs any beamforming gains. Indeed, each GUE's SRS is likely to collide with the SRS of at least one UAV in a neighboring cell in the scenario considered, with said UAV being likely to experience a strong LoS link with the GUE's serving BS.
- Accordingly, the GUE SINR per PRB further degrades when moving from Case 3 to Cases 4 and 5, since the presence of more UAVs in neighboring cells causes the pilot contamination effect to increase its severity.

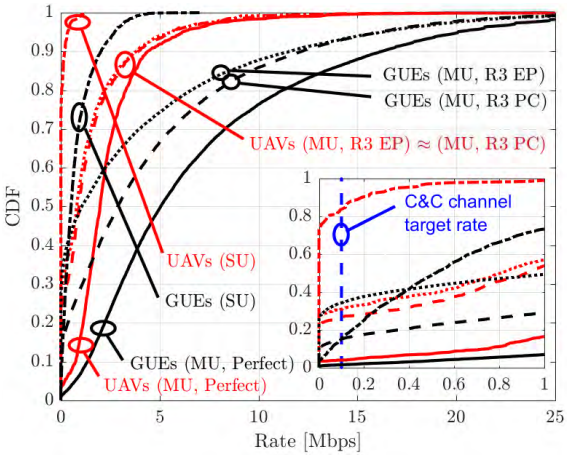


**FIGURE 11.** Rates achieved by UAVs and GUEs in multi-user setups under: *(i)* perfect CSI – "MU, Perfect" (solid), *(ii)* SRS Reuse 3 and UL fractional power control – "MU, R3 PC" (dashed), and *(iii)* SRS Reuse 3 with equal power – "MU, R3 EP" (dotted). The figure also shows the rates in a single-user scenario – "SU" (dash-dot) – and the UAV C&C target rate of 100 kbps (in the enlargement).

### 2) BENEFITS OF MASSIVE MIMO AND UL POWER CONTROL

The ultimate DL rate performance achievable by UAVs and GUEs is shown in Fig. 11 for the 3GPP Case 3, i.e., one UAV and 14 GUEs per sector. This figure not only illustrates the gains provided by massive MIMO networks, but it also highlights the crucial role played by UL power control for CSI acquisition through a comparison of three scenarios: *(i)* perfect CSI ("Perfect"), *(ii)* imperfect CSI obtained through pilot Reuse 3 and fractional UL power control ("R3 PC"), and *(iii)* imperfect CSI obtained through pilot Reuse 3 and equal UL power allocation ("R3 EP"). Fig. 11 motivates us to conclude this section with the following key takeaways:

- Pilot contamination can severely degrade the rate performance of both UAVs and GUEs. Indeed, the median UAV rates attained with imperfect CSI acquisition are reduced to 40% of those achievable without channel estimation errors.
- UL fractional power control does not significantly help to protect the UAV C&C channel. This is because UAVs generally have a strong LoS channel to a large number of BSs, which entails that they are the main source of pilot contamination. As a result, UAVs do not undergo substantial performance gains with UL power control because both their signal and interference powers are similarly reduced. Instead, UL power control is a tremendously helpful tool for GUEs severely affected by pilot contamination, which are those located in the lower tail of the CDF curve. These GUEs benefit from the large power reduction of the UAV-generated SRSs against their more conservative power adjustment.

**TABLE 3. Summary of complementary solutions to improve UAV C&C channel support and UAV-GUE interplay.**

| Solution | Domain | Approach | Challenges/drawbacks |
|---|---|---|---|
| Interference blanking | Time and frequency | Neighboring cells relieve UAVs of DL interference by employing ABSs | Less efficient for high-height UAVs, since they require blanking from large cell clusters |
| Opportunistic scheduling | Time and frequency | Neighboring cells schedule their respective UAVs of different PRBs | Scheduling coordination among cells; less viable for high density of UAVs |
| Fractional pilot reuse | Time, frequency, and space | Conservative pilot reuse for UAVs, more aggressive pilot reuse for GUEs | SRS coordination among cells; larger pilot overhead for high UAV densities |
| Uplink power control | Power | Customize $P_0$ and $\alpha$ in (4), assigning lower values to UAVs than to GUEs | RSRP from many cells may vary fast with high UAV mobility |
| Cooperative MIMO | Space | Suppress interference (CEA precoding) or turn it into useful signal (CoMP) | SRS coordination (CEA precoding); X2 interface between many cells (CoMP) |
| UAV directional antennas | Space | UAV DL C&C signal is strengthened, UL interference to GUEs is reduced | Detrimental for UL of UAVs unless beamforming or antenna selection are possible |

- Massive MIMO boosts the GUEs' data rates. This is due to the multiplexing gain rather than to SINR gain, as illustrated by the non-improving SINRs in Fig. 10. As for the UAV C&C channel, massive MIMO is a key enabler, meeting the target rate of 100 kbps in 74% of the cases even under pilot contamination ("MU, R3 PC").
- Availing of massive MIMO with perfect CSI would allow to achieve said C&C channel target rate in 96% of the cases, as opposed to a mere 16% in single-user scenarios. In order to close the performance gap caused by pilot contamination, one may resort to better pilot assignment and more sophisticated channel estimation and precoding techniques based on multi-cell processing [35], [40], [41]. These approaches leverage in fact channel directionality, which invariably occurs in BS-to-UAV links.

## V. FUTURE OUTLOOK

While massive MIMO provides substantial improvements to UAV cellular communications, one may also use complementary techniques to further improve the performance of UAVs as well as their interplay with traditional GUEs. Table 3 summarizes what we consider to be the most promising solutions, worthy of future research. The remainder of this section is dedicated to an overview of their potentials and challenges. We note that most of the solutions listed rely on the ability of identifying a UAV, which can be accomplished either: *(i)* through mobility and handover history; or *(ii)* with the help of the UAV itself via enhanced measurement report, in-flight mode indication, or altitude information messages [8].

### 1) INTERFERENCE BLANKING

Having understood that the UAV C&C channel performance bottleneck is due to inter-cell interference from a large number of neighboring cells, rather than to a weak carrier signal, one may consider silencing the strongest interfering cells. To this end, the set of strongest interferers could use almost blank subframes (ABSs) on the time-frequency resources that have been assigned to a UAV C&C channel, thus guaranteeing that the latter experiences a satisfactorily high SINR [16], [17]. Determining the sets of BSs that are to use ABSs can have a significant impact on the resultant performance of both UAVs and GUEs. As discussed in Sec. III, the height of a UAV determines the number of strong interfering cells. As a result, the higher the UAV, the larger the number of cells that should protect the UAV C&C channel by undergoing silent phases. This may pose a problem in terms of both the size of the BS cluster to be coordinated and the amount of time-frequency resources to be sacrificed to protect each UAV C&C channel. Thus, this solution may only be suitable for networks with a low density of UAVs.

### 2) OPPORTUNISTIC SCHEDULING

In a massive MIMO network, a more efficient alternative to blanking could be scheduling UAVs on different PRBs. Indeed, part of the benefits brought by massive MIMO to the UAV C&C channel are due to the fact that the neighboring cells of each UAV point most their beams to GUEs, thus focusing most of their radiated power downwards. This can be observed in Fig. 10, where reducing the density of UAVs by a factor of five – i.e., moving from Case 5 to Case 3 – increases by 50% the number of UAVs that achieve the minimum MCS SINR. Such phenomenon suggests that close-by BSs could opportunistically schedule the DL C&C channel of their UAVs on different PRBs, making sure that UAVs are not interfered by other beams pointing upwards in their vicinity.

### 3) FRACTIONAL PILOT REUSE

Both UAVs and GUEs served through a massive MIMO network see their rates increased by orders of magnitude when compared to systems where BSs have a limited number of antennas. Said conclusion holds for networks that employ pilot Reuse 3, and we also showed that these gains can be further boosted if BSs avail of perfect CSI. While allocation of fully orthogonal pilots across the network provides a higher quality CSI, the associated overhead makes this approach infeasible in practical systems. As a trade-off between conservative and aggressive reuse approaches, fractional reuse could

be the most suitable strategy in a network that accommodates UAVs with strong LoS links to a plurality of BSs [42]. Indeed, each BS could selflessly relieve neighboring BSs of severe pilot contamination by assigning a dedicated pool of pilots to its served UAVs, where such pool is agreed beforehand and reused sporadically, e.g., with a reuse factor larger than three. At the same time, each BS could adopt a more aggressive reuse for all remaining pilots, which are assigned to GUEs. As a result, both GUEs and UAVs would be relieved of most pilot contamination, without incurring a large overhead.

#### 4) UPLINK POWER CONTROL

While we showed in Fig. 11 that the effect of pilot contamination can also be alleviated through conventional fractional UL power control, one may also think of more effective techniques. A possible improvement could be achieved by generalizing (4) with customized values of $P_0$ and $\alpha$, e.g., assigning lower values to UAVs than to GUEs, or even accounting for the specific UAV height [43]. A further generalization would involve modifying the approach to account not only for the RSRP from the serving cell but also for the RSRP from neighboring cells. While (4) is thought for a GUE – increasing the transmit power as the GUE's RSRP from the serving BS decreases – this approach may not be always suitable for a UAV. Indeed, when considering a UAV, a decreasing RSRP may be a symptom of a high height. In this case, increasing the power as per (4) would exacerbate the interference generated to a plurality of BSs in LoS. Adapting the power control formula in (4) to account for the RSRP from multiple cells could solve this problem, e.g., by forcing a UAV to reduce its power when the RSRPs from both serving and neighboring cells are low and similar.

#### 5) COOPERATIVE MIMO

One could resort to multi-cell signal processing to boost the UAV C&C channel SINR. In cooperative multipoint (CoMP), a cluster of BSs coherently transmit towards each UAV, aiming to turn interference into useful signal. Despite the promises in terms of rate improvements, CoMP poses a significant overhead over the BS-to-BS X2 interface due to the need of sharing UAV data and achieving a tight symbol-level synchronization [44], [45]. As a more practical alternative, cell-edge-aware (CEA) precoding techniques exploiting inter-cell CSI – acquired through coordinated orthogonal SRSs – may be adopted to steer interference towards the channel nullspace of neighboring UAVs [46]–[48]. While known to be effective for interference management at cell-edge GUEs [49], both CoMP and CEA precoding may face a number of challenges in UAV setups, where the number of sites to be coordinated grows due to the larger number of interfering cells [50], and where the high UAV mobility may entail frequent updates of the coordination clusters.

#### 6) UAV DIRECTIONAL ANTENNAS

While most research efforts have focused on solutions to be implemented at the BS, the 3GPP community is also exploring the possibility of tackling the interference problem directly at the user side, by equipping UAVs with directional antennas. Preliminary contributions have shown that simply implementing a directional antenna without beamsteering capabilities does not provide significant benefits to the DL UAV performance [15]. Moreover, such setup may harm the UL UAV performance, due to the high probability of not pointing the antenna towards the most adequate BS. More encouraging studies argue that antenna selection or beamforming capabilities at the UAV can both enhance the DL C&C signal reception and mitigate the UL interference it generates towards other BSs [51]. However, the latter solution requires increasing the UAV hardware and computational complexity, and it is unclear whether all manufacturers will be willing to implement it.

## VI. CONCLUSIONS

In this article, we took a fresh look at UAV cellular communications, following the most recent trends from the industry, academia, and the standardization fora. Employing realistic 3GPP channel and system models, we evaluated the performance of the downlink command and control channel when supported by either: a traditional cellular network serving one user per transmission time interval, or a multi-user massive MIMO network exploiting spatial multiplexing. Besides comparing the capability and reliability of existing cellular infrastructure to next-generation deployments, we closely examined how aerial users of different heights undergo dissimilar cell selection, carrier signal interference, and pilot contamination. We concluded by discussing complementary procedures that leverage the time, frequency, power, and spatial domains to further enhance UAV cellular communications, and that we believe merit further investigation.

## ACKNOWLEDGMENT

This paper was in part presented at IEEE ICC 2018 [1].

## REFERENCES

[1] G. Geraci, A. Garcia-Rodriguez, L. Galati Giordano, D. López-Pérez, and E. Björnson, "Supporting UAV cellular communications through massive MIMO," in *Proc. IEEE ICC Workshops*, May 2018, pp. 1–6.

[2] *Drones and Aerial Observation: New Technologies for Property Rights, Human Rights, and Global Development—A Primer*, New America, Jul. 2015.

[3] K. P. Valavanis and G. J. Vachtsevanos, Eds., *Handbook of Unmanned Aerial Vehicles*. Amsterdam, The Netherlands: Springer, 2005.

[4] "Unmanned aircraft system (UAS) service demand 2015–2035: Literature review & projections of future usage," U.S. Dept. Transp., Washington, DC, USA, Tech. Rep. DOT-VNTSC-DoD-13-01, Sep. 2013.

[5] M. Mozaffari, W. Saad, M. Bennis, Y.-H. Nam, and M. Debbah. (Mar. 2018). "A tutorial on UAVs for wireless networks: Applications, challenges, and open problems." [Online]. Available: https://arxiv.org/abs/1803.00680

[6] P. Chandhar and E. G. Larsson. (Nov. 2017). "Massive MIMO for drone communications: Applications, case studies and future directions." [Online]. Available: https://arxiv.org/abs/1711.07668

[7] Y. Zeng, J. Lyu, and R. Zhang. (Apr. 2018). "Cellular-connected UAV: Potentials, challenges and promising technologies." [Online]. Available: https://arxiv.org/abs/1804.02217

[8] *Technical Specification Group Radio Access Network; Study on Enhanced LTE Support for Aerial Vehicles (Release 15)*, document 3GPP 36.777, Dec. 2017.

[9] Y. Zeng, R. Zhang, and T. J. Lim, "Wireless communications with unmanned aerial vehicles: Opportunities and challenges," *IEEE Commun. Mag.*, vol. 54, no. 5, pp. 36–42, May 2016.
[10] W. Khawaja, I. Guvenc, D. Matolak, U.-C. Fiebig, and N. Schneckenberger. (Jan. 2018). "A survey of air-to-ground propagation channel modeling for unmanned aerial vehicles." [Online]. Available: https://arxiv.org/abs/1801.01656
[11] S. Hayat, E. Yanmaz, and R. Muzaffar, "Survey on unmanned aerial vehicle networks for civil applications: A communications viewpoint," *IEEE Commun. Surveys Tuts.*, vol. 18, no. 4, pp. 2624–2661, 4th Quart., 2016.
[12] B. Van Der Bergh, A. Chiumento, and S. Pollin, "LTE in the sky: Trading off propagation benefits with interference costs for aerial nodes," *IEEE Commun. Mag.*, vol. 54, no. 5, pp. 44–50, May 2016.
[13] *LTE Unmanned Aerial Aircraft Systems v1.0.1*, Qualcomm Technologies, May 2017.
[14] *New SID on Enhanced Support for Aerial Vehicles*, document 3GPP RP-170779, NTT DOCOMO Inc., Mar. 2017.
[15] *Interference Mitigation for Aerial Vehicles*, document 3GPP R1-1714071, Sequans Communications, Aug. 2017.
[16] *Interference Mitigation for Aerial Vehicles*, document 3GPP R1-1717287, LG Electronics, Oct. 2017.
[17] *Height Parameter and CRS Collision for Aerial Vehicle*, document 3GPP R1-1718267, Sony, Oct. 2017.
[18] *On Interference Detection Schemes and RSRP Statistics for Aerial Vehicles*, document 3GPP R1-1717873, Ericsson, Oct. 2017.
[19] J.-J. Wang, C.-X. Jiang, Z. Han, Y. Ren, R. G. Maunder, and L. Hanzo, "Taking drones to the next level: Cooperative distributed unmanned-aerial-vehicular networks for small and mini drones," *IEEE Veh. Technol. Mag.*, vol. 12, no. 3, pp. 73–82, Sep. 2017.
[20] P. Chandhar, D. Danev, and E. Larsson, "Massive MIMO for communications with drone swarms," *IEEE Trans. Wireless Commun.*, vol. 17, no. 3, pp. 1604–1629, Mar. 2018.
[21] M. M. Azari, F. Rosas, and S. Pollin, "Reshaping cellular networks for the sky: Major factors and feasibility," in *Proc. IEEE ICC*, May 2018, pp. 1–7.
[22] B. Galkin, J. Kibiłda, and L. A. DaSilva. (Oct. 2017). "A stochastic geometry model of backhaul and user coverage in urban UAV networks." [Online]. Available: https://arxiv.org/abs/1710.03701
[23] V. V. C. Ravi and H. S. Dhillon, "Downlink coverage probability in a finite network of unmanned aerial vehicle (UAV) base stations," in *Proc. IEEE SPAWC*, Jul. 2016, pp. 1–5.
[24] E. Kalantari, I. Bor-Yaliniz, A. Yongaçoglu, and H. Yanikomeroglu. (Sep. 2017). "User association and bandwidth allocation for terrestrial and aerial base stations with backhaul considerations." [Online]. Available: https://arxiv.org/abs/1709.07356
[25] A. Garcia-Rodriguez, G. Geraci, D. López-Pérez, L. Galati Giordano, M. Ding, and E. Björnson. (May 2018). "The essential guide to realizing 5G-connected UAVs with massive MIMO." [Online]. Available: https://arxiv.org/abs/1805.05654
[26] S. Euler, H.-L. Maattanen, X. Lin, Z. Zou, M. Bergström, and J. Sedin. (Apr. 2018). "Mobility support for cellular connected unmanned aerial vehicles: Performance and analysis." [Online]. Available: https://arxiv.org/abs/1804.04523
[27] J. Stanczak, I. Z. Kovacs, D. Koziol, J. Wigard, R. Amorim, and H. Nguyen, "Mobility challenges for unmanned aerial vehicles connected to cellular LTE networks," in *Proc. IEEE VTC*, Jun. 2018, pp. 1–5.
[28] *Evolved Universal Terrestrial Radio Access (E-UTRA); Physical Layer Procedures (Release 9)*, document 3GPP 136.213, Jun. 2010.
[29] *Study on Channel Model for Frequencies From 0.5 to 100 GHz (Release 14)*, document 3GPP 38.901, May 2017.
[30] C. U. Castellanos *et al.*, "Performance of uplink fractional power control in UTRAN LTE," in *Proc. IEEE VTC*, May 2008, pp. 2517–2521.
[31] *Further Advancements for E-UTRA Physical Layer Aspects (Release 9)*, document 3GPP 36.814, Mar. 2013.
[32] H. Fattah and C. Leung, "An overview of scheduling algorithms in wireless multimedia networks," *IEEE Wireless Commun.*, vol. 9, no. 5, pp. 76–83, Oct. 2002.
[33] A. Kammoun, H. Khanfir, Z. Altman, M. Debbah, and M. Kamoun, "Preliminary results on 3D channel modeling: From theory to standardization," *IEEE J. Sel. Areas Commun.*, vol. 32, no. 6, pp. 1219–1229, Jun. 2014.
[34] *Physical Layer Aspects for Evolved Universal Terrestrial Radio Access (UTRA) (Release 7)*, document 3GPP 25.814, Sep. 2006.
[35] E. Björnson, J. Hoydis, and L. Sanguinetti, "Massive MIMO networks: Spectral, energy, and hardware efficiency," *Found. Trends Signal Process.*, vol. 11, nos. 3–4, pp. 154–655, 2017.
[36] T. L. Marzetta, E. G. Larsson, H. Yang, and H. Q. Ngo, Eds., *Fundamentals of Massive MIMO*. Cambridge, U.K.: Cambridge Univ. Press, 2016.
[37] *LTE; Evolved Universal Terrestrial Radio Access (E-UTRA); LTE Physical Layer (Release 10)*, document 3GPP 36.201, Jun. 2011.
[38] M. S. Kay, *Fundamentals of Statistical Signal Processing: Detection Theory*. Upper Saddle River, NJ, USA: Prentice-Hall, 1998.
[39] Q. H. Spencer, A. L. Swindlehurst, and M. Haardt, "Zero-forcing methods for downlink spatial multiplexing in multiuser MIMO channels," *IEEE Trans. Signal Process.*, vol. 52, no. 2, pp. 461–471, Feb. 2004.
[40] E. Björnson, J. Hoydis, and L. Sanguinetti, "Massive MIMO has unlimited capacity," *IEEE Trans. Wireless Commun.*, vol. 17, no. 1, pp. 574–590, Jan. 2018.
[41] H. Yin, D. Gesbert, M. Filippou, and Y. Liu, "A coordinated approach to channel estimation in large-scale multiple-antenna systems," *IEEE J. Sel. Areas Commun.*, vol. 31, no. 2, pp. 264–273, Mar. 2013.
[42] L. Galati Giordano *et al.*, "Uplink sounding reference signal coordination to combat pilot contamination in 5G massive MIMO," in *Proc. IEEE WCNC*, Apr. 2018, pp. 1–6.
[43] V. Yajnanarayana, Y.-P. E. Wang, S. Gao, S. Muruganathan, and X. Lin. (Feb. 2018). "Interference mitigation methods for unmanned aerial vehicles served by cellular networks." [Online]. Available: https://arxiv.org/abs/1802.00223
[44] "Cross-link interference management based on Xn support," Nokia, Alcatel-Lucent Shanghai Bell, Tech. Rep. TDoc R1-1711313, Jun. 2017.
[45] A. Lozano, R. W. Heath, Jr., and J. G. Andrews, "Fundamental limits of cooperation," *IEEE Trans. Inf. Theory*, vol. 59, no. 9, pp. 5213–5226, Sep. 2013.
[46] H. H. Yang, G. Geraci, T. Q. S. Quek, and J. G. Andrews, "Cell-edge-aware precoding for downlink massive MIMO cellular networks," *IEEE Trans. Signal Process.*, vol. 65, no. 13, pp. 3344–3358, Jul. 2017.
[47] G. Geraci *et al.*, "Operating massive MIMO in unlicensed bands for enhanced coexistence and spatial reuse," *IEEE J. Sel. Areas Commun.*, vol. 35, no. 6, pp. 1282–1293, Jun. 2017.
[48] A. Garcia-Rodriguez, G. Geraci, L. Galati Giordano, A. Bonfante, M. Ding, and D. López-Pérez, "Massive MIMO unlicensed: A new approach to dynamic spectrum access," *IEEE Commun. Mag.*, vol. 56, no. 6, pp. 186–192, Jun. 2018.
[49] G. Geraci, A. Garcia-Rodriguez, D. López-Pérez, L. Galati Giordano, P. Baracca, and H. Claussen, "Indoor massive MIMO deployments for uniformly high wireless capacity," in *Proc. IEEE WCNC*, Apr. 2018, pp. 1–6.
[50] X. Lin *et al.*, "The sky is not the limit: LTE for unmanned aerial vehicles," *IEEE Commun. Mag.*, vol. 56, no. 4, pp. 204–210, Apr. 2018.
[51] H. C. Nguyen, R. Amorim, J. Wigard, I. Z. Kovács, T. B. Sørensen, and P. E. Mogensen, "How to ensure reliable connectivity for aerial vehicles over cellular networks," *IEEE Access*, vol. 6, pp. 12304–12317, Feb. 2018.

**GIOVANNI GERACI** received the Ph.D. degree in telecommunications engineering from the University of New South Wales, Australia, in 2014. He gained industrial innovation experience at Nokia Bell Labs, Ireland, where he was a Research Scientist from 2016 to 2018. He also held research appointments at the Singapore University of Technology and Design, Singapore, from 2014 to 2015, The University of Texas at Austin, USA, in 2013, Supélec, France, in 2012, and Alcatel-Lucent, Italy, in 2009. Since 2018, he holds a prestigious Junior Leader Fellowship at Universitat Pompeu Fabra, Spain, where he works on wireless communications, networking, and signal processing, with current focus on UAV communications. On these topics, he has co-authored over 50 between book chapters and scientific articles attracting more than 1000 citations, and he is a co-inventor of a dozen EU/U.S. pending patents. He is deeply involved in the research community, being an Editor for the IEEE TRANSACTIONS ON WIRELESS COMMUNICATIONS and the IEEE COMMUNICATIONS LETTERS, a Tutorial Speaker at IEEE WCNC'18, IEEE ICC'18, and IEEE GLOBECOM'18, and a Keynote Speaker at the IEEE PIMRC'18 Workshop on UAV Communications for 5G and Beyond.

**ADRIAN GARCIA-RODRIGUEZ** received the Ph.D. degree in electrical and electronic engineering from University College London, U.K., in 2016. Since 2016, he has been a Research Scientist with Nokia Bell Labs, Ireland, where he focuses on UAV communications and unlicensed spectrum technologies. He organized tutorials at IEEE WCNC 2018 and IEEE ICC 2018 on unlicensed spectrum technologies, and delivered the industrial presentation Drone Base Stations: Opportunities and Challenges Towards a Truly Wireless Wireless Network, which received the Most Attended Industry Program Award at the IEEE GLOBECOM 2017. He was named an Exemplary Reviewer for the IEEE COMMUNICATIONS LETTERS in 2016, and the IEEE TRANSACTIONS ON WIRELESS COMMUNICATIONS and the IEEE TRANSACTIONS ON COMMUNICATIONS in 2017.

**LORENZO GALATI GIORDANO** (M'15) received the M.Sc. and Ph.D. degrees in communication systems from the Politecnico di Milano, Italy, in 2005 and 2010, respectively, and the master's degree in innovation management from IlSole24Ore Business School, Italy. He also spent a part of his Ph.D. as a Marie-Curie Short Term Fellow with the Centre for Wireless Network Design, University of Bedfordshire, U.K., and was a temporary Researcher with the Italian National Research Council. He also has several years of industrial experience as a Consultant at Nokia Siemens Networks, and as an R&D Engineer at Azcom Technology, an Italian SME. He is currently a member of the Technical Staff with Nokia Bell Labs, Ireland. In the last years, he has been contributing to the Nokia F-Cell Project, an innovative self-powered, self-configured, and auto-connected drone deployed small cell powered by a massive MIMO wireless backhaul. F-Cell received the CTIA Emerging Technology (E-Tech) 2016 Award for cutting-edge mobile products and services transforming wide area networks (5G, 4G, and LTE 4.5). Moreover, he has been one of the organizers of the industrial tutorial - *Drone Base Stations: Opportunities and Challenges Towards a Truly "Wireless" Wireless Network*, which received the Most Attended Industry Program Award at the IEEE GLOBECOM 2017.

**DAVID LÓPEZ-PÉREZ** (M'12–SM'17) received the B.Sc. and M.Sc. degrees in telecommunication from Miguel Hernandez University, Spain, in 2003 and 2006, respectively, and the Ph.D. degree in wireless networking from the University of Bedfordshire, U.K., in 2011. He was also a RF Engineer with Vodafone, Spain, from 2005 to 2006, and a Research Associate with King's College London, U.K., from 2010 to 2011. He has done extensive work on cellular small cell and ultra-dense network performance analysis, inter-cell interference coordination and mobility management, has pioneered work on LTE and WLAN interworking, forming part of the team that invented Wi-Fi Boost, which lead to 3GPP LWIP, and is the father of massive MIMO unlicensed (mMIMO-U); a technology that connects the dots among mMIMO and unlicensed spectrum. He is currently a Member of Technical Staff with Nokia Bell Labs and the Lead of the Wireless Stream with the Future Indoor Network Department. He has authored the book *Small Cell Networks: Deployment, Management and Optimization* (IEEE Press/Wiley, 2018), and over 120 book chapters, journal, and conference papers, all in recognized venues. He also holds over 41 patents applications. He received the Ph.D. Marie-Curie Fellowship in 2007, the IEEE ComSoc Best Young Professional Industry Award in 2016, and the IEEE WCNC'18 Best Student Paper Award of the track Wireless Networks in 2018. He was also a finalist for the Scientist of the Year prize in The Irish Laboratory Awards in 2013 and 2015. He has been an Editor of the IEEE TRANSACTIONS ON WIRELESS COMMUNICATIONS since 2016. He was awarded as an Exemplary Reviewer of the IEEE COMMUNICATIONS LETTERS in 2011. He is or has also been a Guest Editor of a number of journals, e.g., the IEEE JOURNAL ON SELECTED AREAS IN COMMUNICATIONS, the IEEE COMMUNICATION MAGAZINE, and the IEEE WIRELESS COMMUNICATION MAGAZINE.

**EMIL BJÖRNSON** (S'07–M'12–SM'17) received the M.S. degree in engineering mathematics from Lund University, Sweden, in 2007, and the Ph.D. degree in telecommunications from the KTH Royal Institute of Technology, Sweden, in 2011. From 2012 to 2014, he held a joint post-doctoral position with the Alcatel-Lucent Chair on flexible radio, Supélec, France, and KTH. He joined Linköping University, Sweden, in 2014, where he is currently an Associate Professor and a Docent with the Division of Communication Systems.

He performs research on multi-antenna communications, massive MIMO, radio resource allocation, energy-efficient communications, and network design. He has authored the textbooks *Optimal Resource Allocation in Coordinated Multi-Cell Systems* in 2013 and *Massive MIMO Networks: Spectral, Energy, and Hardware Efficiency* in 2017. He has been on the Editorial Board of the IEEE TRANSACTIONS ON COMMUNICATIONS since 2017 and the IEEE TRANSACTIONS ON GREEN COMMUNICATIONS AND NETWORKING since 2016. He is dedicated to reproducible research and has made a large amount of simulation code publicly available.

Dr. Björnson has performed MIMO research for more than 10 years and has filed over 10 related patent applications. He received the 2014 Outstanding Young Researcher Award from IEEE ComSoc EMEA, the 2015 Ingvar Carlsson Award, the 2016 Best Ph.D. Award from EURASIP, and the 2018 Marconi Prize Paper Award in Wireless Communications. He also co-authored papers that received best paper awards at the conferences WCSP 2017, IEEE ICC 2015, IEEE WCNC 2014, IEEE SAM 2014, IEEE CAMSAP 2011, and WCSP 2009.